Magnetic field stabilized electron-hole liquid in indirect-band-gap Al$_x$Ga$_{1-x}$As

K. Alberi,[1] B. Fluegel,[1] S. A. Crooker,[2] and A. Mascarenhas[1]

[1]*National Renewable Energy Laboratory, Golden, Colorado 80401, USA*
[2]*National High Magnetic Field Laboratory, Los Alamos National Laboratory, Los Alamos, New Mexico 87545, USA*

An electron-hole liquid (EHL), a condensed liquidlike phase of free electrons and holes in a semiconductor, presents a unique system for exploring quantum many-body phenomena. While the behavior of EHLs is generally understood, less attention has been devoted to systematically varying the onset of their formation and resulting properties. We report on an experimental approach to tune the conditions of formation and characteristics using a combination of low excitation densities and high magnetic fields up to 90 T. Demonstration of this approach was carried out in indirect-band-gap Al$_{0.387}$Ga$_{0.613}$As. EHL droplets can be nucleated from one of two multiexciton complex states depending on the applied excitation density. Furthermore, the excitation density influences the carrier density of the EHL at high magnetic fields, where filling of successive Landau levels can be controlled. The ability to manipulate the formation pathway, temperature, and carrier density of the EHL phase under otherwise fixed experimental conditions makes our approach a powerful tool for studying condensed carrier phases in further detail.

In semiconductors, an electron-hole liquid (EHL) is a Fermi-liquid-like phase of nonequilibrium free electrons and holes that have condensed out of an exciton gas to form macroscopic droplets [1–3]. These interacting carriers remain in a droplet form with an energy distribution described by Fermi-Dirac statistics until they eventually evaporate as excitons or recombine. Consequently, optical absorption and emission spectra contain a wealth of information related to the carrier density and temperature inside the droplet as well as the energy required for excitons to evaporate from the droplet surface (i.e., the work function) [1,4]. EHLs therefore present a prototypical system for spectroscopically studying the behavior of condensed carrier phases. The liquid phase is well known to form under conditions of high exciton densities and low temperatures [1–3]. Often, these conditions are achieved under pulsed optical excitation in indirect-band-gap semiconductors, where the carrier lifetimes are long enough to allow the population to amass beyond the critical concentration for EHL formation. Their behavior has been extensively studied in Si and Ge [1–5] and to a lesser extent in compound semiconductors such as GaP [6], Al$_x$Ga$_{1-x}$As [7,8], and InSb [9,10]. Droplets can grow to be several hundred microns in diameter and can exist for up to tens of microseconds after photocarrier generation has ended. These droplets have also been found to move throughout the semiconductor crystal with high mobility in the presence of strain and exciton concentration gradients as well as in nonuniform electric fields.

The host semiconductor band structure determines the ground state of the EHL and its resulting carrier density. Under conditions that otherwise do not disturb the band structure, the host semiconductor therefore determines the carrier density that can be achieved. The conventional approach of introducing very high exciton concentrations to generate EHL droplets can also immediately overwhelm or bypass intermediate states that provide a pathway to formation. Consequently, it is difficult to alter the EHL formation dynamics and carrier density with such methods.

An alternative approach for forming and studying EHLs would be to excite them with lower-density steady-state sources paired with an extrinsically applied condition that can alter the band structure and thus help to stabilize it. Magnetic fields are one option, and they have been theoretically and experimentally shown to stabilize EHLs under low excitation densities [3,9,11]. This is due to the change in the density of states, which supports higher carrier densities and facilitates a higher electron-hole pair binding energy [3,9]. Although simple demonstrations of EHL stabilization with a magnetic field have been reported [9], variation of both magnetic fields *and* low-density, steady-state optical excitation densities could further be used to gradually tune and study the development and behavior of EHLs with different properties.

Here, we demonstrate the modification of the nucleation conditions and properties of the EHL phase in indirect-band-gap Al$_x$Ga$_{1-x}$As epilayers made possible by a combination of low excitation densities and ultrahigh magnetic fields up to 90 T. Our results show that this approach permits the development of bound multiexciton complex states immediately prior to EHL formation that were not previously observed when EHLs were formed in this system under very high excitation densities [8]. The threshold magnetic field and the exact multiexciton state that acts as the precursor for EHL nucleation is a function of excitation density. Once the EHL phase is formed, we find that its carrier density can be adjusted at very high magnetic fields, ≥ 69 T, by changing the number of Landau levels that are filled. This method of generating the EHL phase therefore provides the ability to tailor the precursor states and properties of the EHL phase for further study of the link between properties and behavior in multielectron systems.

Electron-hole liquid formation was studied in an undoped, 400 nm thick Al$_{0.387}$Ga$_{0.613}$As epilayer grown by molecular beam epitaxy. The alloy composition was determined through a combination of reflective high-energy electron diffraction and high-resolution x-ray diffraction measurements to an uncertainty of $\Delta(x) = \pm 0.003$. This sample was previously found to have an indirect band gap, with the X conduction-band minimum located 5 meV below the Γ conduction-band minimum at zero magnetic field [12,13]. The indirect band gap was also verified to remain indirect upon the application

of high magnetic fields [13]. Residual dopant impurity concentrations are present at the 10^{13} cm^{-3} level. Magneto-photoluminescence (PL) measurements were carried out in superfluid helium at 1.6 K using both the 60 T long pulse and 100 T multishot magnets at the National High Magnetic Field Laboratory at Los Alamos National Laboratory [14,15]. The 2 s pulse duration of the 60 T magnet is sufficiently long to permit continuous PL measurements through the entire pulse. The 100 T magnet pulse duration is shorter (only tens of milliseconds from 40 to 100 T), such that we only use one PL spectrum acquired at peak field [15]. The magnetic field was oriented along the [001] crystal direction of the sample (the Faraday geometry), and PL spectra were continuously acquired in 3.5 and 1.5 ms intervals, respectively, in the two magnets. A continuous-wave, 515 nm solid-state laser was used as the excitation source, and the unpolarized beam was delivered to the sample through a 550 μm diameter optical fiber coupled directly to the sample. Unpolarized PL was collected through the same fiber, ensuring that the majority of the collected PL originated in the same area as the optical excitation. This last point is noteworthy, since EHL droplets can migrate, and this configuration ensures that the spectra were measured from the droplets within the vicinity of the highest excited carrier densities. Excitation densities ranging from 30 mW/cm^2 to 17 W/cm^2 were controlled with neutral density filters. We expect little lattice heating at these injection levels.

Figure 1 shows the PL spectra in 1 T increments up to 58 T for four different excitation densities (30 mW/cm^2, 300 mW/cm^2, 3 W/cm^2, and 17 W/cm^2). In all cases, a bound-exciton (BE$_X$) peak [12] is prominent in the low-magnetic-field range of 0–10 T. Owing to the high exciton reduced mass at the X point ($\sim$0.23m_0 compared to 0.07m_0 at the Γ point), the bound-exciton peak does not undergo a substantial diamagnetic shift. This peak disappears as another peak, labeled 1, grows in intensity with increasing field followed by a second peak at lower energy, labeled 2. One of two overall effects then occurs. At the two lowest excitation densities [Figs. 1(a) and 1(b)], peak 1 dominates the spectra at all magnetic fields. Peak 1 remains relatively stationary under the excitation density of 30 mW/cm^2, but at 300 mW/cm^2, it starts to broaden, overtake peak 2 and shift to lower energies at the highest magnetic field. At the two highest excitation densities [Figs. 1(c) and 1(d)], however, peak 2 grows in intensity, broadens and shifts to lower energy with increasing magnetic fields. Its width, its intensity relative to peak 1, and the extent of the redshift in its peak energy with increasing field all depend on the excitation density, as determined by comparing the evolution of the spectra in Figs. 1(c) and 1(d). Trends in the peak energies with magnetic field are shown in Fig. 2 for clarity, and they immediately highlight the distinction between these two behavioral regimes. This graph also includes measurements made out to 90 T at intermediate excitation densities of 100 mW/cm^2, 1 W/cm^2, and 10 W/cm^2.

We will now discuss the origins of the emission peaks 1 and 2. First, we note that peaks 1 and 2 always first arise with a narrow linewidth, and they then broaden after some threshold combination of magnetic field and excitation density. The narrow and fully broadened forms of each peak correspond to emission from two different phases, but their linewidth and peak energy appear to evolve continuously. We will therefore
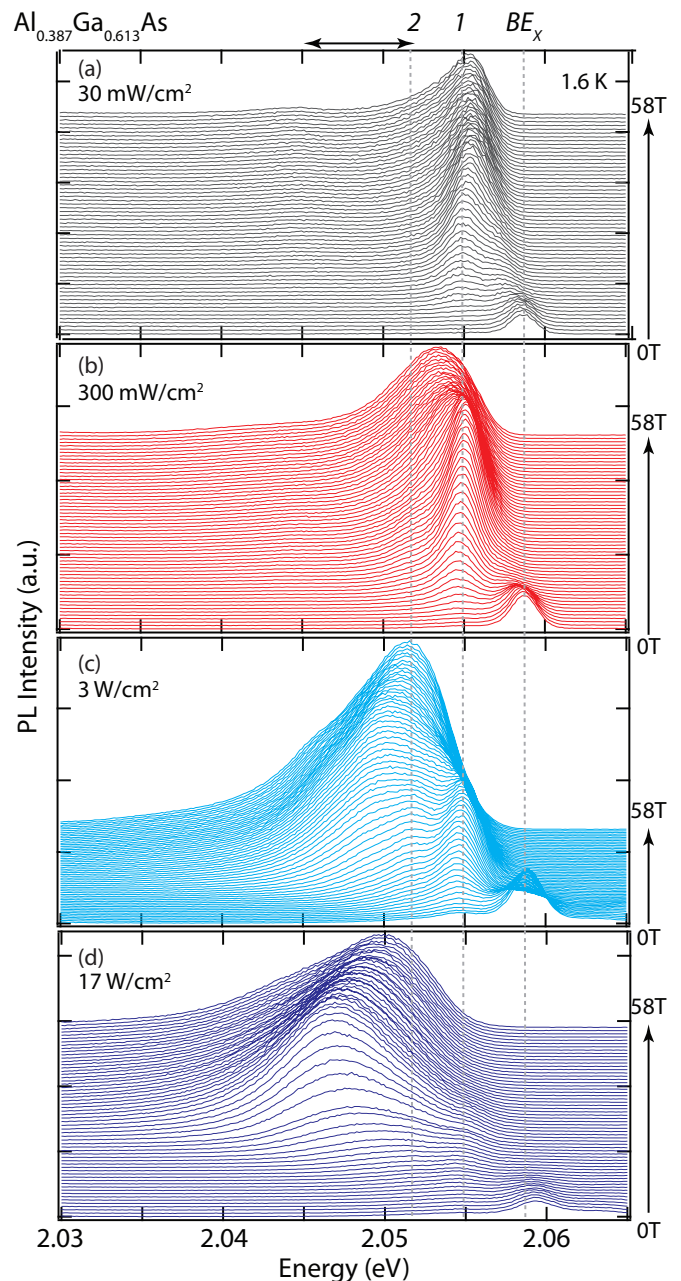

FIG. 1. Magneto-PL spectra of Al$_{0.387}$Ga$_{0.613}$As measured at 1.6 K under four different excitation densities (30 mW/cm^2, 300 mW/cm^2, 3 W/cm^2, and 17 W/cm^2). The spectra are plotted in 1 T increments up to 58 T. The dashed vertical lines mark the energies of the BE$_X$, 1, and 2 peaks at low fields and excitation densities.

refer to these peaks as 1 and 2 for both the narrow and broadened manifestations. The distinguishing feature between them is whether they first arise (at low magnetic fields, $\leqslant$10 T) at $\sim$2.0546 eV (peak 1) or $\sim$2.052 eV (peak 2), as shown in Fig. 2.

We propose that at their inceptions, the narrow peaks 1 and 2 arise due to the creation of bound multiexciton complexes. Biexcitons and multiexciton complexes bound to neutral impurities can be considered as precursors or intermediate states to the EHL phase. They have been found to form at
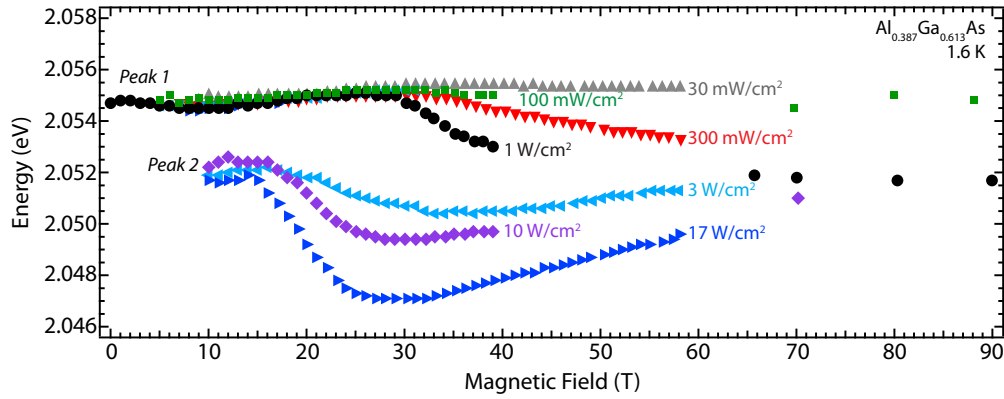
FIG. 2. Energies of peaks 1 and 2 measured $Al_{0.387}Ga_{0.613}As$ at 1.6 K as a function of magnetic field for seven different excitation densities.

impurities at zero magnetic field in lightly doped Si crystals and emit a series of narrow PL peaks between the single bound-exciton and EHL emission peaks [3,16]. Biexcitons were also recently observed in direct-band-gap $Al_{0.3}Ga_{0.7}As$ at zero magnetic field under low power excitation [17]. The energetic splitting between the exciton and biexciton lines in that case was ~2.5 meV. The spacings that are presently observed between the BE_X peak and peaks 1 and 2 are approximately 4.3 and 7.1 meV, respectively. These higher binding energies can be expected in indirect-band-gap semiconductors. Additionally, their linewidths are similar to that of the BE_X peak, indicating transitions from distinct bound states. Narrow emission linewidths are typical of multiexciton complexes in other semiconductor systems [16]. While no spectral signatures of multiexciton states were observed during previous investigations [7,8] of EHL formation in $Al_xGa_{1-x}As$, the pulsed excitation powers used in those measurements were high enough to substantially exceed the free-exciton threshold for EHL formation. The authors of Ref. [8] noted that the fast EHL formation times in $Al_xGa_{1-x}As$ allow droplets to nucleate directly from an electron-hole plasma phase [8]. Additionally, magnetic fields were found to stabilize the formation of multiexciton complexes bound to impurities in direct-band-gap InSb, where they otherwise would not be observed at zero field [9,18]. Such evidence of multiexciton states in Si, $Al_xGa_{1-x}As$, and InSb with similar emission behavior to peaks 1 and 2 before broadening therefore supports our assignment. We will refer to these two multiexciton complex states as $m = 1$ and $m = 2$ (for narrow peaks 1 and 2).

Once broadened, peaks 1 and 2 are associated with emission from the EHL phase. Emission from EHL droplets is typically characterized by very broad peaks at energies below the free-exciton and BE_X emission peaks. Qualitatively, the line shape, peak width, and the redshift from the BE_X peak all resemble those of EHL emission in indirect-band-gap $Al_xGa_{1-x}As$ at zero magnetic field [8]. However, in order to definitively assign PL emission to the EHL phase (rather than the exciton gas or electron-hole plasma phases), one must first determine the carrier density and temperature through spectral line-shape fitting and then generate a phase diagram for that system. Quantitatively, we show that these broadened peaks 1 and 2 arise from the EHL phase using the zero-field phase diagram for indirect-band-gap $Al_xGa_{1-x}As$ reported in Ref. [8]. The ground-state energy E_G of the EHL system is a summation

of three contributions: the kinetic energy of noninteracting particles E_0; the Hartree-Fock exchange energy E_{exch}; and a correlation energy E_{corr}. Each of these terms is dependent on the electron-hole density in the liquid, n, which is defined by the minimum of E_G [3]. The electron-hole density can be experimentally determined from the spectral PL line shape. Generally, the line shape of the PL peak associated with the EHL phase can be described by the following function [1,4,7]:

$$I_{EHL}(hv) = I_0 \int_0^{hv'} dE\, D_e(E) D_h(hv' - E) f(E, E_F^e, T_{EHL})$$
$$\times f(hv' - E, E_F^h, T_{EHL}), \quad (1)$$

where E_F^e and E_F^h are the electron and hole Fermi energies, respectively, $E_F = E_F^e + E_F^h$, D_e and D_h are the density of states in the conduction and valence bands, respectively, f is the Fermi function, and T_{EHL} is the electron-hole temperature. hv' is expressed as

$$hv' = hv - E_g + E_X + \varphi + E_F, \quad (2)$$

where E_g is the indirect-band-gap energy, E_X is the exciton binding energy, and φ is the work function. The summation of the last four terms in Eq. (2) constitutes the renormalized band gap E_g'. Finally, a state-broadening term Γ is usually included in the expression of the density of states to better fit the low-energy tail [19].

In our case, the fitting must account for the presence of Landau levels in the joint density of states. We used the same general approach outlined by Stormer and Martin [5]. The large band gap of $Al_{0.387}Ga_{0.613}As$ allows the conduction- and valence-band densities of states to be calculated separately according to the framework set forth by Luttinger [20]. A few example spectral fits are shown in Fig. 3(a). The values of E_g', n, and T_{EHL} extracted from the broadened peaks 1 and 2 are shown in Figs. 3(b)–3(d). This includes peak 2 generated under excitation densities ≥ 3 W/cm² and magnetic fields ≥ 20 T. Peak 1 in the spectra generated under excitation densities ≤ 1 W/cm² started to broaden at much higher magnetic fields. Thus, data points from spectra measured at fields ≥ 30 T and ≥ 69 T for excitation densities of 1 W/cm² and 100 mW/cm², respectively, were also included. Above 30 T, n exceeds the critical density ($n_c = 2 \times 10^{18}$ cm⁻³) and T_{EHL} is below the critical temperature ($T_c = 34$ K) for EHL formation reported in Ref. [8] for indirect-band-gap $Al_xGa_{1-x}As$ at zero magnetic
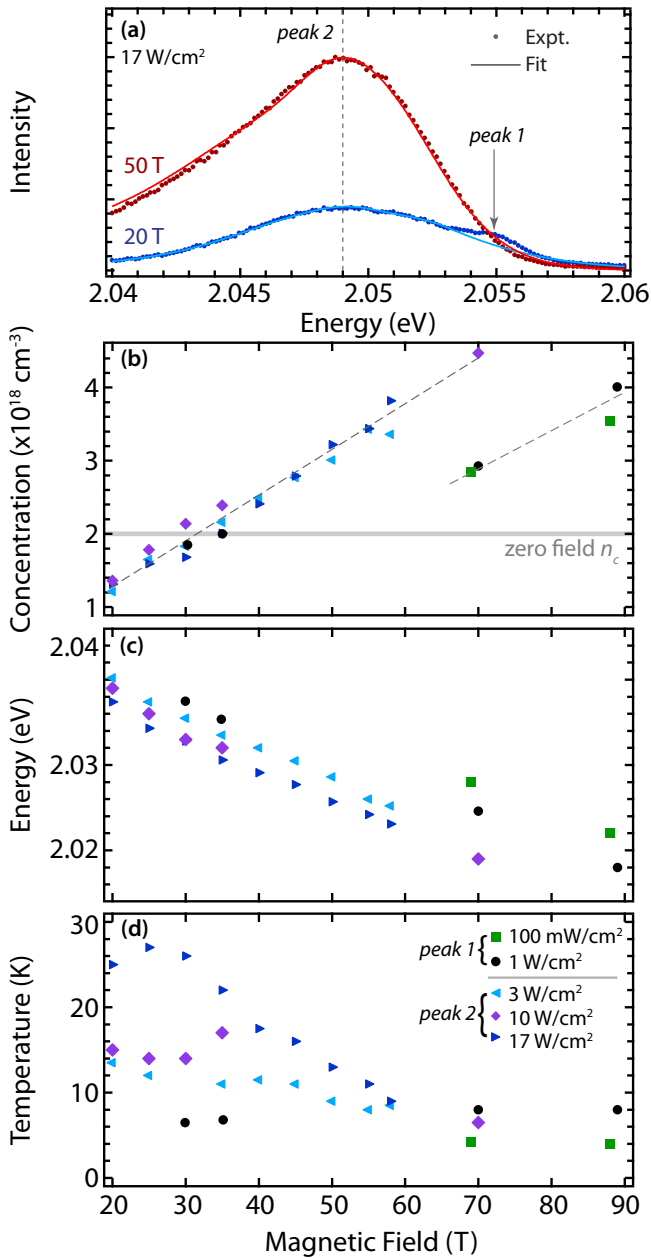
FIG. 3. (a) Example fits to spectra obtained at 20 and 50 T under an excitation density of 17 W/cm^2. (b)–(d) EHL parameters extracted by PL line-shape fitting: (b) electron-hole concentration n; (c) renormalized band gap E'_g; (d) electron-hole temperature T_{EHL}.

field. T_{EHL} also decreases with increasing n, which is another signature of EHL behavior [8]. Line-shape fitting therefore supports our conclusion that the fully broadened peaks are associated with emission from the EHL phase.

Rapid broadening of peaks 1 and 2 on the low-energy side indicates that the EHL forms via fast growth in n directly from the multiexciton complex precursor states $m = 1$ and $m = 2$, respectively. Such a rise in n is aided by a redistribution of the density of states into Landau levels, which leads to a reduction in E_0 and E_G [5]. It is particularly interesting to note that the EHL evolves directly from either the $m = 1$ or $m = 2$ states at nonzero magnetic fields instead of those states acting merely as independent entities between the free exciton

and the EHL [16]. We can understand the dependence on the excitation density by first assuming that the $m = 2$ state has a higher number of bound excitons than the $m = 1$ state and that the binding energy per exciton is lower in the $m = 2$ state, per the framework outlined by Sauer in Ref. [16]. It is then expected that the EHL phase would be stabilized first at the $m = 2$ state due to the ability of the magnetic field to overcome its lower exciton binding energy. However, since the density of the $m = 2$ states is lower than the density of $m = 1$ states, there will be some minimum excitation density needed to sustain the $m = 2$ state. Below this, the EHL will be forced to form out of the more populous $m = 1$ state. The higher binding energy of those excitons will subsequently require a higher magnetic field to stabilize the EHL phase, which is exactly what we observe experimentally.

Besides originating from different multiexciton complex states, the EHL parameters from these two regimes behave somewhat differently as a function of magnetic field. Generally, and in accord with previous findings in Ge [5,21] and InSb [9], n rises with magnetic field [Fig. 3(b)], which in turn causes a further reduction in the renormalized band-gap energy [Fig. 3(c)]. The values of n extracted from the broadened peak 2 generated at excitation densities $\geqslant 3$ W/cm^2 are the same within the error of the fits, regardless of the excitation density. The electron-hole densities of the EHLs associated with the broadened peak 1 generated at 1 W/cm^2 also match those values at magnetic fields 30–35 T. However, at higher magnetic fields, ≥ 69 T, the EHL droplets associated with the broadened peak 1 have a much lower n than those associated with peak 2. This is qualitatively confirmed by comparing the spectra measured at 69–70 T under excitation densities of 100 mW/cm^2, 1 W/cm^2, and 10 W/cm^2, shown in Fig. 4. The widths of the peaks generated under the two lower excitation densities are similar to one another, but are much smaller than that generated under the highest excitation density.

Once the EHL has formed, one might expect that n should be independent of its original precursor state. This appears to be the case for the EHLs stabilized at magnetic fields below 40 T. A possible explanation for the discontinuity at magnetic fields ≥ 69 T could be a difference in the filling of valence-band Landau levels between the two excitation regimes. Theoretical
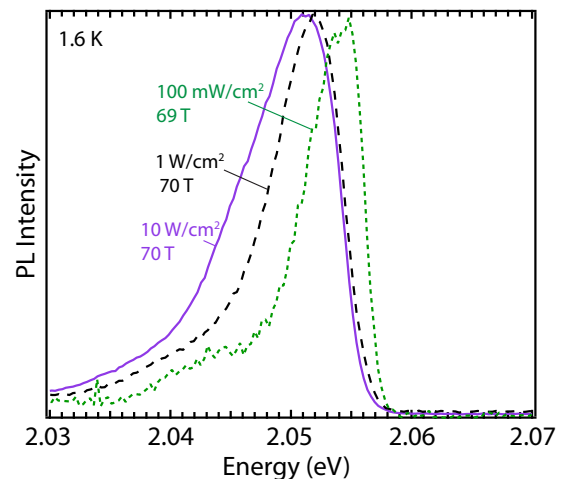

FIG. 4. PL spectra measured at 69 T (100 mW/cm^2) and 70 T (1 W/cm^2 and 10 W/cm^2).
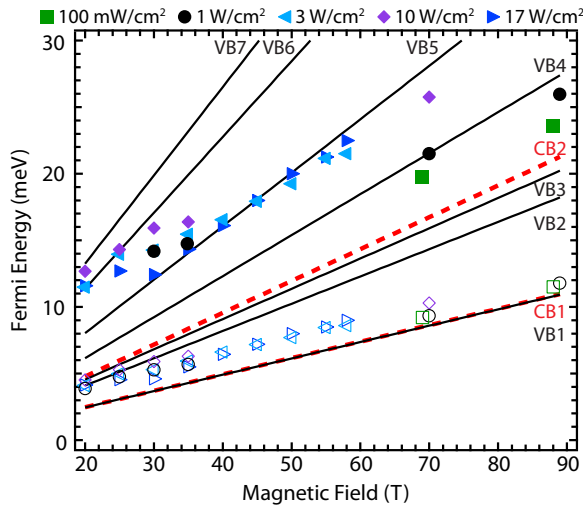
FIG. 5. Conduction band (dashed lines) and valence band (solid lines) Landau-level energies as a function of magnetic field, as well as electron (open symbols) and hole (solid symbols) Fermi energies derived from spectral line-shape fitting.

calculations by Skudlarski and Vignale [22] suggest that filling a new Landau level will cause an irregularity in the kinetic energy and thus in the total ground-state energy of the EHL. This will consequently result in a discontinuous change in n. Figure 5 shows that at such high magnetic fields, one less Landau level in the valence band is filled at the two lowest excitation densities at magnetic fields ≥ 69 T. Our observation of a clear discontinuity in n provides experimental confirmation of this theoretically predicted phenomenon, and is made possible by our use of steady-state excitation, which allows the carriers to more readily thermalize to the global energy minimum, as well as the use of high magnetic fields, where the discontinuity is predicted to be greater [22] and can be more readily detected.

The small offset in E'_g between the EHL phase generated under the different excitation densities could be due to a difference in droplet radius R which will affect the extent of the band-gap renormalization [23]. The magnitude of band-gap renormalization depends on R^2, and thus larger droplets will undergo a greater renormalization. For example, the difference in the absolute E'_g between 3 and 17 W/cm² is ∼2 meV, which is consistent with expected changes in droplet size for $Al_xGa_{1-x}As$ [8].

The other interesting effect to note is the difference in T_{EHL} [Fig. 3(d)] between the excitation densities. Previous reports of EHLs formed at high magnetic fields in Ge and InSb indicated that the temperature of the EHL is independent of the field strength. This appears to be approximately true for the EHLs generated at $\leqslant 3$ W/cm², where only a small change in T_{EHL} occurs over the entire field range. Yet T_{EHL} of the fully formed EHL decreases rapidly with magnetic field when higher excitation densities are used. The temperature reduction could be caused by magnetic-field-induced carrier cooling, which has been observed previously in electron-hole systems due to enhanced relaxation via electron-phonon coupling [24,25]. Immediately after photogeneration, hot electrons rapidly thermalize to T_{EHL} via emission of optical phonons. The relaxation rate is known to decrease with increasing carrier population, which is consistent with our finding of a higher T_{EHL} in the EHL generated under an excitation density of 17 W/cm² compared to 3 W/cm² [26,27]. The application of a magnetic field and appearance of Landau levels alters the energy relaxation rate due to phonon emission [24]. Increased splitting between Landau levels, and the population of only the lowest Landau levels in this case, reduces the probability of inter-Landau-level scattering by optical phonons, but intralevel scattering by acoustic phonons becomes more prevalent [24,25,27]. Thus, cooling of the carrier temperature within the EHL is attributed specifically to enhanced acoustic-phonon emission. The temperatures of the EHLs generated under the range of excitation densities appear to converge around ∼60 T.

In summary, we have demonstrated that the formation and properties of an EHL phase can be tuned using low excitation densities and magnetic fields up to 90 T. Our results suggest that the EHL phase can develop from one of two multiexciton complex states depending on the excitation density. At low magnetic fields, the electron-hole density of the EHL is the same, regardless of the nucleation state. However, at high magnetic fields, the electron-hole density differs based on whether it formed from the $m = 1$ or $m = 2$ multiexciton complex. We attribute this difference to the filling of one less Landau level at low excitation densities $\leqslant 1$ W/cm². Redistribution of the density of states within the Landau levels with increasing magnetic field is also responsible for the enhancement of acoustic-phonon-assisted cooling in EHLs formed under the highest excitation densities. The simultaneous influence of both the excitation density and magnetic field on the properties of the EHL phase suggest that these tools can be used together to tune condensed carrier phases and further study their behavior in detail.

[1] Ya. Pokrovskii, Phys. Status Solidi A **11**, 385 (1972).

[2] C. D. Jeffries, Science **189**, 955 (1975).

[3] L. V. Keldysh and P. N. Lebedev, Contemp. Phys. **27**, 395 (1986).

[4] T. K. Lo, Solid State Commun. **15**, 1231 (1974).

[5] H. L. Stormer and R. W. Martin, Phys. Rev. B **20**, 4213 (1979).

[6] D. Bimberg, M. S. Skolnick, and L. M. Sander, Phys. Rev. B **19**, 2231 (1979).

[7] E. Cohen, M. D. Sturge, M. A. Olmstead, and R. A. Logan, Phys. Rev. B **22**, 771 (1980).

[8] H. Kalt, K. Reimann, W. W. Ruhle, M. Rinker, and E. Bauser, Phys. Rev. B **42**, 7058 (1990).

 [9] I. V. Kavetskaya, N. V. Zamkovets, N. N. Sibeldin, and V. A. Tsvetkov, J. Exp. Theor. Phys. **84**, 406 (1997).

[10] R. D. Grober and H. D. Drew, Phys. Rev. B **43**, 11732 (1991).

[11] S. T. Chiu, Phys. Rev. B **9**, 3438 (1974).

[12] B. Fluegel, K. Alberi, J. Reno, and A. Mascarenhas, Jpn. J. Appl. Phys. **54**, 042402 (2015).

[13] K. Alberi, A. V. Mialitsin, B. Fluegel, S. A. Crooker, J. L. Reno, and A. Mascarenhas, Appl. Phys. Express **7**, 111201 (2014).

[14] S. A. Crooker, D. G. Rickel, S. K. Lyo, N. Samarth, and D. D. Awschalom, Phys. Rev. B **60**, R2173 (1999).

[15] S. A. Crooker and N. Samarth, Appl. Phys. Lett. **90**, 102109 (2007).

[16] R. Sauer, Phys. Rev. Lett. **31**, 376 (1973).

[17] F. Sarti, M. Matutano, D. Bauer, N. Dotti, S. Bietti, G. Isella, A. Vinattieri, S. Sanguinetti, and M. Gurioli, J. Appl. Phys. **114**, 224314 (2013).

[18] N. N. Sibeldin, Phys.-Usp. **46**, 971 (2003).

[19] R. W. Martin and H. L. Stormer, Solid State Commun. **22**, 523 (1977).

[20] J. M. Luttinger, Phys. Rev. **102**, 1030 (1956).

[21] M. S. Skolnick and D. Bimberg, Phys. Rev. B **21**, 4624 (1980).

[22] P. Skudlarski and G. Vignale, Phys. Rev. B **47**, 16647 (1993).

[23] H. Kalt, J. Lumin. **60-61**, 262 (1994).

[24] R. W. J. Hollering, T. T. J. M. Berendschot, H. J. A. Bluyssen, H. A. J. M. Reinen, P. Wyder, and F. Roozeboom, Phys. Rev. B **38**, 13323 (1988).

[25] Yu. V. Zhilyaev, V. V. Rossin, T. V. Rossina, and V.V. Travnikov, Sov. Phys.-JETP **72**, 692 (1991).

[26] K. Kash and J. Shah, Appl. Phys. Lett. **45**, 401 (1984).

[27] S. E. Esipov, M. Msall, and J. P. Wolfe, Phys. Rev. B **47**, 13330 (1993).